Publications of the Astronomical Society of the Pacific
105: 1308–1321, 1993 November

A Multiobject Fiber Spectrograph for The Hale Telescope

DONALD HAMILTON,[1] J. B. OKE,[2] M. A. CARR,[3] J. CROMER, F. H. HARRIS,[4] J. COHEN, E. EMERY,[5] AND L. BLAKEE[5]

Palomar Observatory, California Institute of Technology, Robinson Laboratory MS 105-24, Pasadena, California 91125
Electronic mail: hamilton@astrosun.tn.cornell.edu, oke@dao.nrc.ca

Received 1993 March 1; accepted 1993 August 5

ABSTRACT. A new faint-object spectrograph has been designed around the capabilities of fiber optics. This instrument, the Norris Spectrograph, is for exclusive use at the Cassegrain focus ($f/16$) of The Hale Telescope and is optimized for faint galaxy spectroscopy. There are 176 independently positionable fibers that are serially manipulated by a single robotic system. Each of these fibers sees 1.6 arcsec on the sky and the total positionable area is in excess of 300 arcmin^2. Unlike most multiobject spectrographs which utilize fibers that are several tens of meters long, the philosophy of the design of the Norris was quite the antithesis, i.e., to minimize the fiber lengths; hence, it is an entirely self-contained telescope-mounted instrument for the Cassegrain focus. The instrument consists of an integrated xy stage, for the fiber positioning, and an attached optical spectrograph. The design of the spectrograph is basically classical: spherical collimator mirror, standard reflection grating, and a newly designed all-transmissive-optics camera lens. The detector currently used is a thinned, AR-coated 2048×2048 Tektronix CCD. Fibers are arranged in two linear opposing banks that can access the 20 arcmin diameter field-of-view (FOV) of the instrument. The accuracy of fiber placement (assuming errorless coordinates) is less than 0.1 arcsec over the entire FOV. Fibers may be placed as close as 16 arcsec. This permits close pairings of fibers for very faint-object spectroscopy. Beam switching between paired fibers, as was done with two-channel spectrographs of yesteryear, will help average out temporal and spatial variations of the light of the night sky. Actual observations performed in this mode of operation indicate that the quality of the sky subtraction improves, as would be expected. The density of paired fibers within the Norris FOV matches the approximate density of faint field galaxies expected to a blue magnitude of 21. Software exists to take object lists (α,δ) and convert them to rectilinear (x,y) values (mm) on the xy stage by gnomonic projection and to assign fibers. This software also corrects for precession of the equinoxes, proper motion if epoch differences exist, and corrects for differential atmospheric refraction. To place a single fiber takes approximately 5 s on the average. A lower limit to the efficiency of the spectrograph plus telescope has been estimated to be 6.8% at 5500 Å. In order to derive the throughput of the instrument, the efficiency of the telescope, estimated to be approximately 56%, must be divided out. This value is consistent with the expectation that the reduction in efficiency from that of a standard CCD spectrograph such as The Hale Telescope's Double Spectrograph will be about a factor of 2. This results from the 60%–70% transmittance of the fibers and other losses. The spectra produced are linear with little distortion. With 10 Å spectral resolution, fitting residuals on the order of 100 km s^{-1} are easily obtainable by modeling the dispersion by a third-order polynomial. The resolutions currently available range from 1 to about 20 Å. The spectra have a FWHM in the direction perpendicular to that of the dispersion of about 90 μm, or equivalently about three 27 μm pixels found in the older Tektronix 2048 CCDs. The interorder spacing of 250 μm is large enough to permit clean spectrum extractions. The instrument has been in use for several years. The scientific programs vary from high resolution (1 Å resolution) spectroscopy of stars in nearby globular clusters to a low spectral resolution (10 Å) survey of faint field galaxies. In this latter survey, with typical 2-hr exposures, absorption-line redshifts as high as $z\sim0.5$ have been routinely measured. Several heretofore unknown quasars with redshifts around three have also been discovered serendipitously.

1. INTRODUCTION

The popularization of the use of fiber optics for astronomical spectroscopy has manifested itself at Palomar Observatory with the design, construction, and successful use of the Norris Spectrograph. This multiobject spectrograph is capable of observing up to 176 separate objects at a single time, thus greatly improving the observing efficiency of The Hale Telescope for large astronomical surveys that have been long a mainstay of research at Palomar. Originally the instrument was designed to be used nearly exclusively for field galaxy redshift surveys. Nevertheless, a number of other distinctly different programs such as studies of globular clusters in external galaxies and observa-

[1]Also, Cornell University, Center for Radiophysics and Space Research, Space Sciences Bldg., Ithaca, NY 14853-6801.
[2]Now at Dominion Astrophysical Observatory, 5071 W. Saanich Road, Victoria, B.C. V8X 4M6.
[3]Now at Princeton University, Peyton Hall, Princeton, NJ 08540.
[4]Now at U.S. Naval Observatory, Flagstaff, AZ 86002.
[5]Retired.

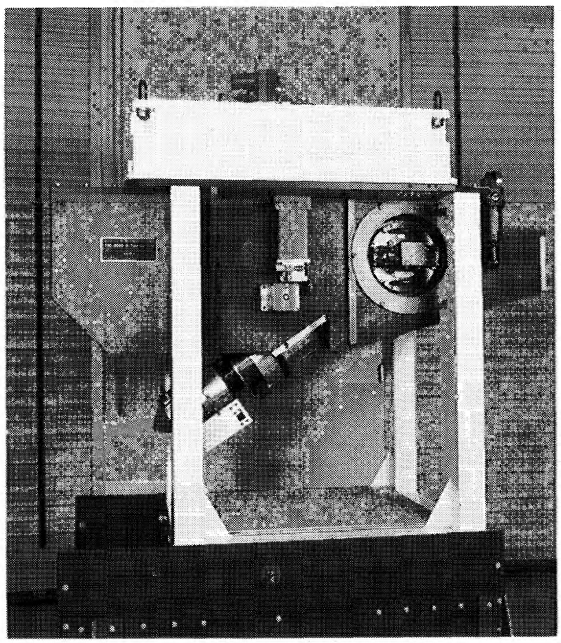

FIG. 1—Photograph of the side view of the Norris Spectrograph showing the grating rotator, the slow-scan CCD guider and its transfer optics, the camera lens barrel with the CCD Dewar attached, and the encoder gas purge regulator (to the far right). Figure 2 outlines the major outer components of the instrument, some which can be seen in this photograph.

tions of faint stars in globular clusters have been conducted with the Norris Spectrograph. A side view photograph of the instrument on its handling carts is given in Fig. 1 and a schematic view of the instrument is given in Fig. 2. The instrument as built was first described in Hamilton (1990), which included a discussion of the full echelle mode of the instrument, which as yet, has not been implemented.

The particular optical configuration of the Cassegrain focus of The Hale Telescope is advantageous for a fiber spectrograph. The near-flat focal plane is large and the Cassegrain cage is spacious enough to accommodate an integrated instrument, i.e., both positioning stage and spectrograph as part of the same assembly. The large scale (390 μm per arcsec) of the Cassegrain focus is useful in permitting fibers to come relatively close to one another on the sky. Faint-object spectroscopy requires sampling the sky around a target object as closely and simultaneously (temporally) as possible. This is not possible with most fiber spectrographs as the plate scale tends to be too small thus precluding closely spaced pairs of fibers (one for object plus sky and one for sky only) unless there is a dedicated sky fiber, but this introduces other complications.

The basic optical configuration of the instrument was set when three parameters were chosen. These were (1) the angular sampling of each fiber on the sky; (2) the input focal ratio of the fiber, and (3) the demagnification of the collimator/camera system. The rationale behind our choice of the first two of these parameters is given herein below. The decision regarding the demagnification of the spectrograph involves many inputs. Without discussion here, the resultant number is two.

The first parameter, that of the fiber size projected onto the sky, was determined by a simple calculation as to the size of the aperture that would maximize the contrast between the light of a typical faint galaxy[6] and that of the measured night sky over Palomar Mountain. The calculated size is less than 1 arcsec which is, in practical terms, too small for several reasons. The first and foremost consideration, is that the seeing at the 200-in. telescope is rarely better than 1 arcsec which implies substantial "slit losses" even if a 1 arcsec aperture is used.

Positional inaccuracies such as those found in the object astrometry or those created by telescope guiding imperfections would also increase the loss of signal for such a small aperture. However, based upon extensive experience, object coordinates good to 0.2 arcsec are obtainable, albeit through straightforward tedium. This source of error was not considered to pose a problem. A second source of positional inaccuracy will be in telescope jitter during the guided exposures. These are at the level of at least 0.5 arcsec (both random and systematic) and could be larger. A third source of positional inaccuracy will be in the model for the conversion of right ascension and declination into xy stage coordinates. The principal errors in this transformation will be the inaccuracies of the coefficients in the model which are the scales (arcsec per mm) in each of the two directions and the rotation angle between (x,y) and (α,δ).

Lastly, for such a small aperture the effects of differential atmospheric refraction could be significant for even small zenith distances. Due to these complications, an input aperture (defined by the fiber core size) was chosen to be 1.6 arcsec. For some observational programs a larger aperture is desired. We are in the process of designing auxiliary optics that can be straightforwardly inserted on short notice to alter the input focal ratio so that the projected fiber size on the sky is increased to a diameter of $\sim$2.5 arcsec.

The second parameter to be set, that of the fiber input focal ratio, was determined through extensive testing of various fibers. In many instruments that match fibers to an existing spectrograph, the effects of focal ratio degradation (the output beam width is greater than that of the input beam) would reduce the instrumental étendue. However, the design of the Norris Spectrograph basically obviated such a problem as the collimator focal ratio was matched to the measured fiber output focal ratio. Additional discussion regarding fiber pecularities can be found in Sec. 2.2. Additional reading on the pre-Norris status of fiber optics in astronomy may be found in the A.S.P. Conference Proceedings, *Fiber Optics in Astronomy* (Barden 1988).

[6]As would be expected, the determination of the maximum contrast aperture is dependent upon the particular form for the profile of the objects to be observed. Instead of assuming a model profile, we used an averaged profile of field galaxies found on good seeing, deep CCD frames. These galaxies that contributed to the profile are typical ones expected to be observed with the Norris.

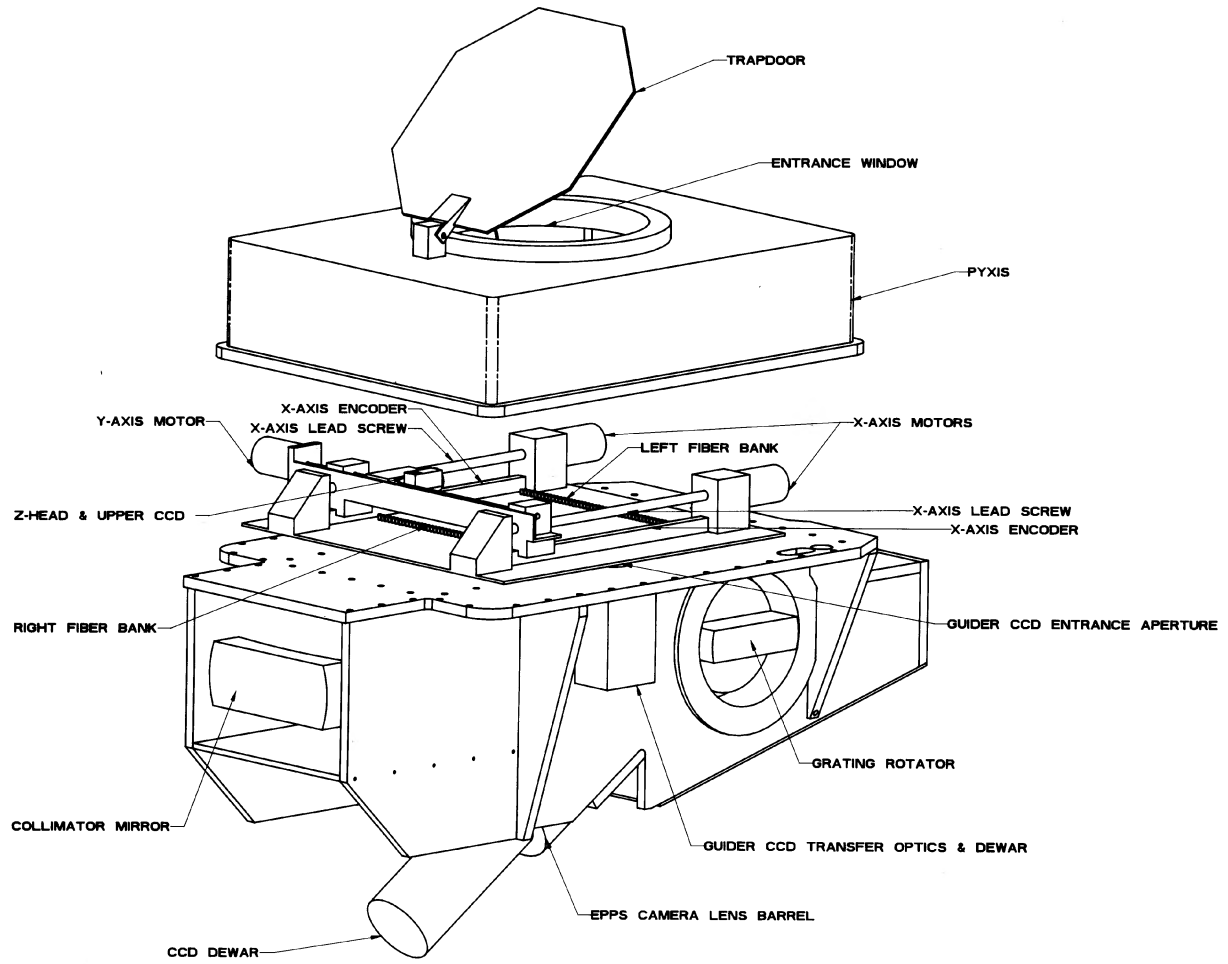

FIG. 2—A schematic of the main parts of the instrument.

2. OPTICAL TRAIN

The optical configuration, diagrammed in Fig. 3, consists of focal reduction transfer optics (lenslet/prism), 2.1 m of fiber whose output is collimated by a spherical mirror, dispersed by a reflection grating, and focused onto a thinned, AR-coated Tektronix CCD by an all-transmissive-optics camera lens designed by Epps. Each of these components will be discussed below.

Fiber optics have the unfortunate, but not insurmountable problem that they do not preserve entropy, i.e., the angular distribution of light is increased. For large telescopes that are being used with fibers it is necessary to minimize the increase in entropy, also called focal ratio degradation (FRD),[7] in order to maximize efficiency and spectral resolution. The $f/16$ focal ratio at the Cassegrain focus of the 200-in. telescope is too slow for straightforward fiber operations. A series of tests were made of fiber efficiency as a function of the input focal ratio and the output focal ratio. The tests showed that an output focal ratio of about $f/4$ would be ideal if the input focal ratio was about $f/6$ to $f/8$. The output focal ratio of $f/4$ would allow a very simple collimator design. An input focal ratio of $f/4.5$ in air or, equivalently $f/6.7$ in quartz, was achieved by using focal reduction optics in the fiber head itself.

2.1 Focal Reduction Optics (Lenslet/Prism)

As mentioned above it was necessary to reduce the focal ratio of the incoming beam at the Cassegrain focus with transfer optics. An additional requirement for these transfer optics was that the light path would have to be redirected at ~90 deg with respect to the telescope optical axis to properly feed the fiber. The basic design was of a simple $f/3$ rod lens with a radius of curvature of 3 mm. This lens, when combined with a prism face which allowed total internal reflection, formed a combination which changed the focal ratio from $f/16$ to $f/6.7$ (in quartz) and rotated the beam by approximately a right angle. The fiber was then optically coupled to the output face of the prism to elimi-

[7]An excellent discussion of focal ratio degradation may be found in Ramsey (1988).

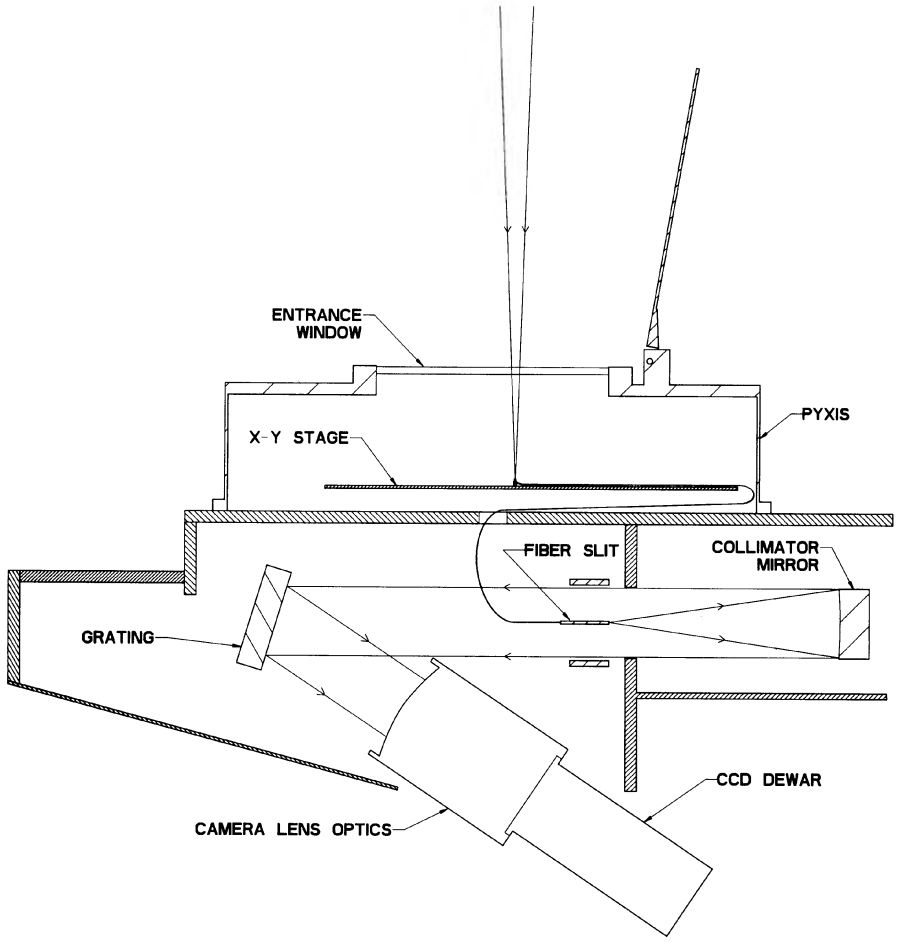

FIG. 3—The optical train of the instrument.

nate any light loss at the interface. With this focal reduction the fiber core diameter of 185 μm, which is the field stop, converts to 1.56 arcsec. Spherical aberration introduced by this lens is insignificant (18 μm) at the entrance to the fiber. A schematic cutaway drawing of the lenslet/prism encased in the fiber head is given in Fig. 4.

These lenslet/prisms were manufactured out of fused silica and all surfaces polished by Cosmo Optics of Middleton, NY. The front refracting surface is also coated with a single layer of magnesium fluoride for maximum transmittance at 5500 Å. Each one of the lenslet/prisms is cemented into a brass envelope using Norland #61 optical cement. This envelope also holds the samarium–cobalt magnet. A small hole in the envelope provides access to the output end of the lenslet/prism to which the fiber is optically coupled. The stainless-steel tube that contains the fiber is cemented to the brass envelope on the outside. The cement used to fasten both the magnet and the stainless-steel tube onto the brass envelope was 3M Structural Epoxy.

2.2 Fibers

In order to select the appropriate fiber for the Norris Spectrograph extensive testing was carried out on a variety of fibers. The tests involved transmittance measurements as a function of the input focal ratio for both blue and red light, focal ratio degradation, and microbending effects. Ideally, the transmittance of the fibers should be high from the near UV to the far red. Some control over this transmittance is possible through the hydroxl content of the fiber core which is introduced by hydrogenation during the drawing process. Wet fibers, which have a high hydroxl content, are advantageous for good near-UV throughput. However, the absorptivity from OH absorption features in the red and far-red regions is greater. In dry fibers, the low OH content does lower the near-UV transmittance, and, concomitantly the effect of the OH overtones is low.

One of the distinct advantages of using short fiber lengths, as in the Norris Spectrograph, is that the internal fiber losses such as those from the OH overtones become less important. Wet fibers, therefore, will be appropriate for the short lengths that we are considering. Another distinct advantage in the use of short fibers is that the effects of microbending on the output focal ratio is reduced. Based upon the results of the tests, fibers manufactured by Polymicro were selected. A special order was placed for fibers with a fused silica core with a diameter of 185 μm, a clad-

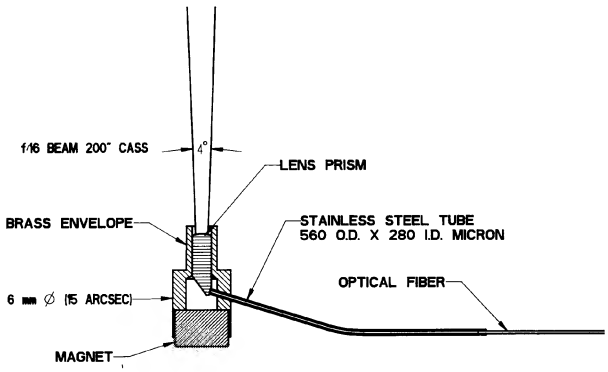

FIG. 4—A cutaway schematic of the fiber head showing the position of the lenslet/prism, the samarium–cobalt magnet, the fiber in its protective stainless-steel tubing, all of which are encased in the brass envelope. The proper focus for the telescope is at about the lower part of the lenslet/prism.

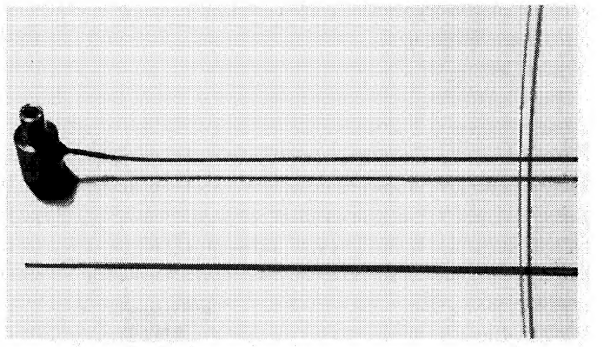

FIG. 5—A photograph of a completed fiber showing the fiber head and the stainless-steel tubing that protects the ends of the fibers. Both the stainless-steel tubing and the fiber were polished to optical flatness.

ding with a diameter of 220 μm, and coated with a polyimide buffer with a diameter of 240 μm.

Each fiber used in the spectrograph was first cut to a length of about 2.1 m and each end was cemented into 280/560 μm (ID/OD) stainless-steel hypodermic tubing (#304 drawn). At the input end of the fiber, the stainless-steel length was about 300 mm and at the output end the length was only about 100 mm. A photograph of a completed fiber is given in Fig. 5. The epoxy used was Epok-Tek 353 ND. This type was chosen because of its low shrinkage. At each end, only about 1 to 2 mm of the fiber length was coated with epoxy and slowly drawn into the tube. It was felt that if too much epoxy was used then the fiber would act as a wick and draw a considerable amount of epoxy into the tubing. Too much epoxy or the wrong type of epoxy can increase stress on the fiber which might reduce the throughput. After the epoxy was thoroughly cured, the fibers and the tubing were then polished at both ends. The polishing was continued until, upon examination at high magnification of the ends, there were no imperfections discernable to the eye.

As alluded to in the Introduction, the ability to successfully obtain a realistic sky spectrum for a particular faint object is directly correlated with the spatial proximity of the sky aperture to the object aperture as well as the temporal sampling frequency. The optical configuration of Cassegrain focus of The Hale Telescope is particularly advantageous in this regard as the large scale permits the fiber heads to be placed rather close together. Given the 6 mm base of the fiber head (due to the size of the Sa–Co magnet), and some additional area as an adequate safety zone, the fibers may be placed as close as 16 arcsec.

The fiber-to-fiber throughput variations at a fixed wavelength are approximately 15% minimum to maximum. Enough spare fibers were made so as to allow only those with the highest throughput to be installed into the instrument. The remaining interfiber variations are straightforwardly removed by our flat-fielding procedures.

2.3 Fiber Slit

The output ends of the fibers are brought together in a plane to form what is in effect a long slit. The fiber ends were arranged along the curved focal surface of the spherical collimator. This assembly that holds the fiber ends was designed to minimize obscuration and has a cross section of 5 mm out of a beam width of 150 mm. The fibers were fed underneath the xy stage and entered the spectrograph portion of the instrument from the side. The fibers go through about a 100 mm radius of curvature bend so as to face the collimator. A slow bend such as this one does not compromise the integrity of the fiber system.

2.4 Collimator Mirror

A spherical collimator with a focal length of 625 mm and dimensions of 150×406 mm^2 was cut out of a polished Zerodur mirror. Custom Optics of Tucson Arizona did the optical work. In retrospect, some other commonly used mirror blank material, such as BK7, would have provided a better match to the expansion coefficient of aluminum. The design is basically that of a classical Schmidt camera, but correctorless. At $f/4$ the uncompensated spherical aberration is insignificant compared with the projected fiber output size. The polished surface was coated with silver and then overcoated with a single layer of silicon monoxide for maximum reflectivity at 5500 Å. For this phase of the instrument, in which only wavelengths redward of 4000 Å are to be observed, silver is the appropriate choice.

2.5 Gratings

The grating is located at the center of curvature of the spherical collimator, that is, at the position of the corrector in a Schmidt camera. Standard reflection gratings made by Milton–Roy (formerly Bausch and Lomb) used in the Double Spectrograph are also used in the Norris Spectrograph. The size of the ruled area is 154×203 mm^2. The collimator to camera angle is 35 deg.

The gratings are mounted in cells that are easily attached to the grating rotator assembly (described in Sec. 3.4). There are a variety of gratings with constants that

vary from 158 to 1200 ℓmm^{-1}. The lowest dispersion currently available is 4.9 Å pixel^{-1} and the highest is 0.32 Å pixel^{-1}.

2.6 Camera Optics

Traditionally the choice for a spectrograph camera is some variant of a Schmidt system. The manufacturing techniques are well known and straightforward. These camera systems were appropriate as long as the detector was small. CCDs such as those made by TI obstructed little of the collimated beam so the overall efficiency of the system remained high. However, with modern CCDs of the size like the Tektronix 2048 with 27 μm pixels, a high-efficiency Schmidt camera would have been large and expensive. Alternatives were sought in the form of all-transmissive camera systems. Epps designed an excellent camera lens for use with the Keck Low-Resolution Imaging Spectrograph (Epps 1990), and this system was adopted for the Norris Spectrograph as well.

The camera has a focal length of 305 mm and a focal ratio of $f/1.35$. This camera yields an essentially[8] flat focal plane with a field diameter of 75 mm. The design was optimized for wavelengths between 3800 and 10,000 Å and minimized the longitudinal chromatic and spherical aberrations. The rms spot size for white light is 32 μm on-axis and slightly better off-axis. This size is quite adequate given that the projected size of the fiber onto the detector is about 90 μm.

The camera consists of four lens groups of one, three, two, and one elements each. It is basically a Petzval portrait lens (von Rohr 1899) but with the addition of the triplet inserted between the fluorite singlet and the doublet for aberration reduction. A cross section of the lens schematic with several ray paths indicated is given in Fig. 6. The last element is a classical fused silica field flattener. A flat CCD Dewar window made out of fused silica and 6.35 mm thick was incorporated into the design so as to properly take into account the spherical aberration introduced by this element. The surfaces are spherical with the exception of two that are strongly aspherical. The deviation from sphericity amounts to about a thousand waves at maximum so canonical spherical comparison techniques such as Hindle's sphere would be inadequate or expensive. However, these types of tests were supplanted by measurements made with a profilometer originally designed for use with the Keck secondary mirror. The first and third elements are made out of fluorite and both of these elements were polished by Janus Optics from boules grown by Optovac, Inc. Janus Optics also coated the singlet lens. The remaining optical surfaces were polished by Pardahlan of the Lick Optical Shop. The complex barrel was designed by Carr and fabricated at Caltech. The whole lens and barrel were assembled by Lick and Palomar personnel. A cross-sectional view of the lens barrel which holds the camera lens sans field flattener is presented in Fig. 7. (The field flattener is part of a different, much simpler assembly.)

[8]The focal plane sag from center to a radius of 40 mm is about 60 μm.

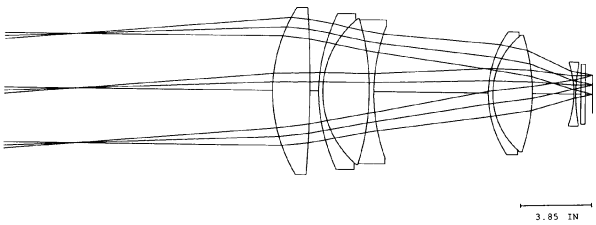

FIG. 6—A schematic of the optical layout of the Epps camera lens used in the Norris Spectrograph. Ray paths are drawn indicating those elements that contain the most power. The first and third elements are made out of fluorite (calcium fluoride). The last two elements, that of the field flattener and the CCD cryostat window, are made out of fused silica. The remainder of the glasses of the lens are noted in Fig. 7.

The camera lens is sealed within the lens barrel which has an AR-coated fused quartz entrance window (basically plane parallel) at an angle of 10 deg with respect to the axis. There are several gas purge ports on the lens barrel that not only allow pressures to equilibrate, but also for purging with dry nitrogen gas. Some care is needed with fluorite as it is hydroscopic.

Although the details of the characteristics of the lens have been given by Epps (1989), these were not for the lens as built. As this design is sufficiently advanced, a brief discussion of the performance of the lens seems in order. The various measured radii of curvature and thicknesses were input to the optical analysis program CODE V. The refractivities of the various elements were taken from the melt data provided by the glass manufacturers.

Ray aberration curves for the final as-built lens, assuming best element alignment, used in the Norris are presented in Figs. 8 and 9. Aberration plots are given for each of three field angle positions 0, 2.5, and 5 deg, in three different wavelengths 4000, 4800, and 6000 Å, and for tangential (Fig. 8) and sagittal (Fig. 9) fans of rays. The aberration in micrometers is plotted on the ordinate and

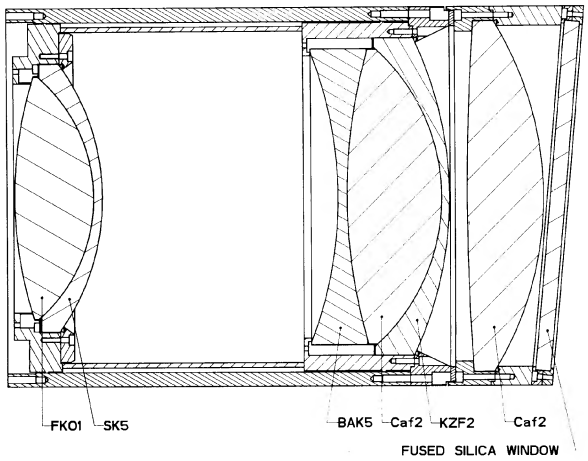

FIG. 7—A cutaway drawing of the principal part of the Epps lens encased in its barrel. This barrel contains purge ports not only to allow the pressure to equilibrate, but also to permit the inside of the barrel to be flushed with dry N_2 gas to protect the hydroscopic fluorite elements. The diameter of the barrel is about 25 cm.

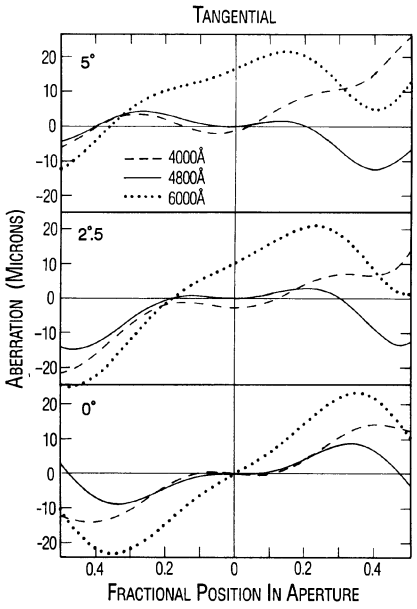

FIG. 8—Transverse aberration plots for a tangential fan of rays for the camera lens of the Norris Spectrograph. The ordinate is the aberration in micrometers and the abscissa is the position of the entering ray in the aperture (here taken as the aperture stop). There are three curves for each panel, one for each of the indicated wavelengths. These plots are presented for three field angles of 0 (on axis), 2.5, and 5 deg. The shapes of the curves are indicative of the type of aberration that principally contributes.

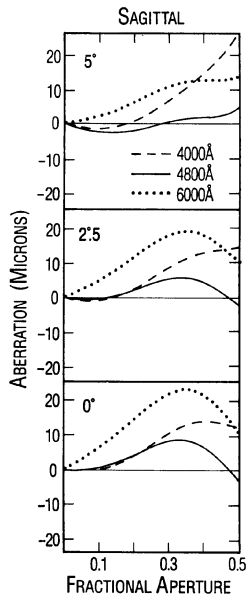

FIG. 9—Same type of aberration ray plots as in Fig. 8, but for sagittal fans of rays.

the value of the abscissa represents the fractional aperture position within the aperture stop of the entering ray. For the nonaxial fields, all of the plots of the tangential fans of rays at all wavelengths, suggest that the principal residual aberrations are due to overcorrected zonal spherical aberration and to lateral color. In all cases, the deviations are less than 25 μm which is essentially one pixel.

In the CODE V model of the lens, the various elements were assumed to be properly centered within 25 μm. However, realistic mechanical centering tolerances are closer to 50 μm, with centering being established from the centration of the rim of the element. The effect on the lens' performance of nonaligned elements was investigated by decentering each element in the model by at most 50 μm. The increase in the spread of light at the best focus amounted to less than a few percent of the smallest spot size attainable. This is a negligible effect.

However, the predominant effect of decentration of the elements was to increase the distortion of the system. Figure 10 is a plot of the distortion predicted by the models, assuming centered elements. The distortion of a decentered system has a functional form quite distinct from that of this curve and increases with the amount of net decentration. The distortion of the assembled lens has been measured to be 0.2% at an angle of 2.3 deg, which is just slightly larger than that of the centered lens. This result is indicative that the elements are near their best alignment.

Focusing of the spectrograph is done by moving the collimator mirror and not the elements of the camera lens. The positions of the lens groups are fixed relative to one another. With the use of the CODE V model, it was realized that focusing can also be accomplished by moving the field flattener, CCD Dewar window, and the detector relative to the rest of the lens.

The astigmatic field curves for the lens are presented in Fig. 11 for both sagittal and tangential fans of rays. There is a slight defocus due to the curved focal plane which is unfortunately in the opposite direction from the curved surface of a thinned Tektronix 2048 CCD which has a center that is closer to the secondary of the telescope than its periphery.

2.7 Comparison Lamps

Comparison lamps of neon, mercury, argon, and incandescant were placed near the *xy* stage below the entrance

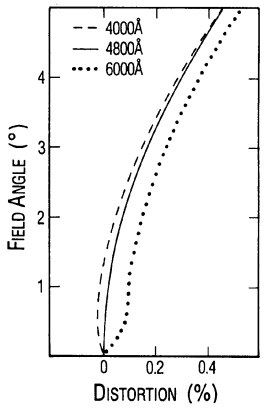

FIG. 10—Presented is the distortion predicted for the Epps lens based upon the CODE V model with centered elements. The measured distortion is 0.2% at a field angle of 2.3 deg. The agreement between the measured and expected distortions suggest that the lens elements are near their best centrations.

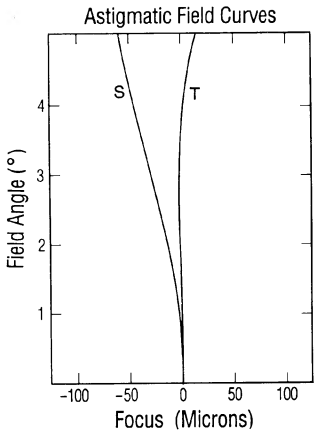

FIG. 11—This plot shows the focal curves for both sagittal (labeled with an *S*) and tangential (labeled with a *T*) fans of rays for the Epps camera lens. The ordinate is the field angle in degrees and the abscissa is the deviation from paraxial focus in micrometer.

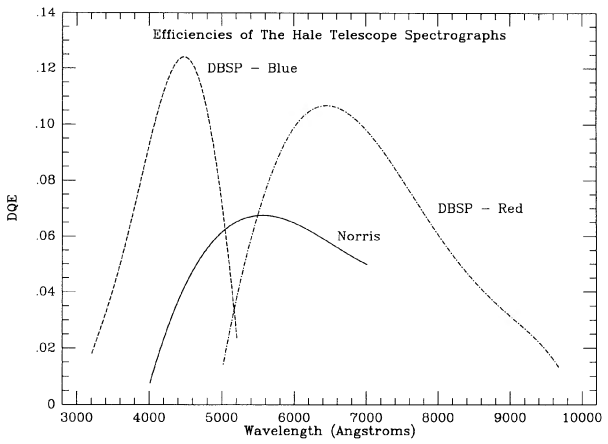

FIG. 12—The efficiency of the Norris Spectrograph plus telescope derived from observations of the standard star BD+17 4708 using a 300 ℓmm^{-1} grating blazed at 5000 Å. Standard atmospheric extinction over Palomar was assumed, which is an underestimate given that the observation was about four months after the Mt. Pinatubo eruption. In addition, the seeing was rather poor ($\sim$2 arcsec) for the photometric night, and the efficiency has been corrected by a factor 1.8 based upon a model of the fractional throughput under these conditions. See the text for the details of the seeing correction, which is also an underestimate. This correction allows a proper and direct comparison with the Double Spectrograph (also shown) which is its only purpose in presenting it in this particular form.

apertures to the fibers. The light from these lamps is reflected off a screen placed on the underside of the trapdoor (see Sec. 2.8 for more discussion). There is an interlock system such that the trapdoor must be closed in order for the lamps to be powered. This is to prevent the lamps from being activated at unwanted times.

It is anticipated that flat-field calibration exposures will be taken with the stage prepared in the same manner as for the object exposures and using the normal flat-field system that is in place at the prime focus cage of the 200-in. telescope. Additional calibration exposures that are normally taken are of the twilight sky and undithered quartz for tracing of the spectra for the determination of the extraction parameters. (Dithered flat-fielding procedures are described in Sec. 3.3.)

2.8 Entrance Window and Trapdoor

In order to keep the *xy* table, rails, lead screws, etc., clean from dust and debris an entrance window was placed at the top of the instrument. This window allows the instrument to be approximately hermetic to help preserve optical coatings. The window is protected by a trapdoor that is manipulated by gearing to a Compumotor stepper motor and it is remotely controlled by the instrument computer.

The window is made out of pure fused silica (Dynasil 4000 grade) and was polished to within a few tens of waves of flatness by Custom Optics. The window is 520 mm in diameter and 10 mm in thickness. The window is coated with a single layer of magnesium fluoride, optimizing the throughput for 5500 Å.

2.9 Instrument Efficiency

A lower limit to the efficiency of the instrument has been measured by the observation of the Palomar standard star BD+17° 4708 during a photometric night. The observations were done through a fiber of typical transmittance. Unfortunately the seeing for the observation was rather poor, being $\sim$2 arcsec. The overall efficiency using a 300 ℓmm^{-1} grating blazed at 5000 Å is presented in Fig. 12 along with that of the Double Spectrograph (taken directly from Oke and Gunn 1982). Both of these measurements are of the combined spectrograph plus telescope efficiencies. The latter is estimated to be $\sim$56%. The dramatic falloff in the efficiency of the Norris Spectrograph at the bluer wavelengths is due primarily to the CCD employed for those particular observations (another AR-coated, thinned TEK CCD).

This efficiency measurement for the Norris Spectrograph is an underestimate for two reasons. First, the atmospheric extinction over Palomar assumed was that of a pre-Pinatubo era. This assumption will introduce a systematic underestimate of the true efficiency and this effect could be as much as 25%. The other underestimate originates from seeing losses due to our rather small input aperture of 1.6 arcsec. In order to make a proper comparison with that of the Double Spectrograph, which used a 10 arcsec wide slit, the derived efficiency was increased by a factor of 1.8 due to the $\sim$2 arcsec seeing. This factor was estimated by modeling the seeing profile with a Gaussian of similar width and calculating the fractional loss using a 1.6 arcsec aperture. The resultant overall efficiency, with a steady atmosphere, is within the errors as to what is predicted based upon knowing the losses of each of the optical elements.

3. MECHANICS

This section describes the main mechanical components of the Norris Spectrograph. It is in this area that the in-

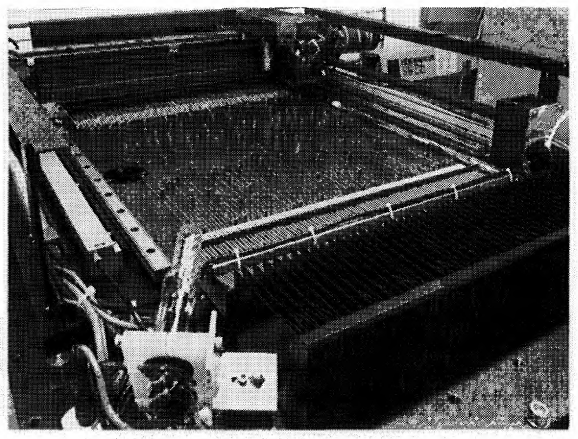

FIG. 13—A photograph of the *xy* stage arranged for an actual field.

strument has its greatest complexity. All of these components are under computer control and each will be discussed. A schematic of the instrument and its main components is given in Fig. 2.

3.1 *XY* Stage

The heart of the Norris Spectrograph is the *xy* stage onto which 176 independently positionable fiber heads may be placed. The stage consists of rectilinear *x* and *y* motions upon which rides the fiber pickup head. A photograph of the *xy* stage, without the instrument cover being present, is given in Fig. 13. Some of the fibers have been placed according to an actual setup for field galaxy observations. The active staging area is about 500×500 mm^2.

The *x* axis is defined by two high accuracy grade (about 1 μm rms) rails (manufactured by THK) that bracket the fiber staging area and upon which glides the *y* gantry assembly. The rails are coated for permanent lubrication with the dry penetrant Dichronite. At one end of this assembly is the quadruple lead thread for the 3 mm pitch Teflon-coated lead screw which defines the *x* motion. Although the pitch of the lead screw is 3 mm, the quadruple lead thread increases the effective pitch to 12 mm. This clearly reduces the accuracy possible, but there is a significant increase in the rigidity and strength of the lead screw. All the lead screws used in the *xy* stage were manufactured by Kerk Motion Products, although the equivalent manufactured by DSA (California) would have been a better choice.

The *x* axis lead screw is directly coupled to a Compumotor AX 83-135 microstepping motor. Compumotor microstepping motors are used throughout the instrument. Compumotors can be easily programmed—only ASCII strings are required for motor control. These motors have 12,800 microsteps per revolution, and with an effective screw pitch of 12 mm one microstep translates into 1 μm. The measured accuracy is about 4 μm which is a combination of all the inaccuracies involved. This level translates to 0.01 arcsec—more than adequate for our purposes. The major inaccuracy in placing a fiber will be the errors in the coordinates of the object. The *y* axis is designed similar to the *x* axis except that a less robust lead screw and a smaller stepper motor were used (Compumotor AX 83-93). The guide rail is the same as that used for the *x* axis. The perpendicularity of the *x* and *y* axes is good to one part in 50,000.

Positional information for each axis is obtained by the use of 620 mm long glass scale incremental linear encoders manufactured by Heidenhain (model LS 403). The resolution of these encoders, increased by a factor of 4 by electronic division, is such that one encoder step is equivalent to 1 μm. These encoders have worked successfully in subfreezing temperatures. As a precaution against false readings due to dirt accumulating on the glass scales of the encoders, there is a pressure regulated dry nitrogen gas purge system that includes a multistage filtering system to remove oil and other particles from the bottled gas.

A magnetic brake was installed on each of the *xy* stage stepper motors. These brakes are designed to prevent the motion of the screws at undesired times. They are configured so that when the power is removed the brakes are engaged. Power to both the stepper motors and the brakes is removed when the *xy* stage is not being used. The brakes were manufactured by Empire Magnetics.

The platform onto which the fiber heads are placed is a 6 mm thick steel plate overcoated for rust prevention. In addition, a layer of Teflon tape was placed on the active area to aid in cushioning the fiber head placement. This layer also serves to reduce the effective magnetization of the fiber head which was slightly larger than necessary. There is no lateral slippage of a fiber head at any position of the *xy* stage (even vertical) due to this ostensibly slick surface. The tape also helps protect the *xy* stage from possible corrosive elements such as Los Angeles air.

The maximum travel distance for a fiber being carried straight out from its stowed position is 280 mm. This is about 25 mm beyond the center line between the two fiber banks. These limits imply that fibers from opposing banks can overlap in the center 50 mm (about 2 arcmin) of the stage. The area of highest fiber density is, therefore, 2×20 arcmin. In actual setups, overlapping fibers occur routinely, but more commonly when objects of high central concentration are observed, which is not often.

The fibers may be moved laterally, under certain circumstances, up to an angle of 10 deg from a line perpendicular to their stowed positions. Such strong skewing of the fibers is rarely needed as the number of objects that are centrally concentrated is vanishingly small when compared with the near random distribution of faint galaxies for which the Norris Spectrograph was designed to observe.

3.2 Fiber Pickup Head

Riding on the *y* axis which moves upon the *x* axis is the fiber pickup or *z* head. This mechanical device grabs the neck of the fiber head using a precision three point collet. The lifting mechanism consists of a pinion that is attached to the shaft of a Compumotor AX 57-51 motor. This pinion drives a rack attached to a vertical sliding assembly

(sleeve) which holds the collet. The high-precision (~ 5 μm) collet was specially manufactured by Hardinge to our tolerances. The collet movement is actuated by a Ledex rotary solenoid and by spring loading the connecting arm the default state is closed. The collet and its actuating mechanism are placed within a sleeve and are completely free to rotate about the z axis.

The procedure to pick up a fiber is to first energize the solenoid to open the collet. The stepper motor is then rotated a fixed number of microsteps and the collet will have enveloped the neck of the fiber head. The power to the solenoid is removed and the collet closes. The stepper motor reverses direction and the fiber head is lifted from the xy table. Unless there is some external force that moves a fiber head, the z head always finds its fiber. In order to sense the presence of a fiber within the collet, an infrared LED and photodiode are placed such that the line between the two will be intersected by the fiber head.

3.3 Collimator Focus and Dithering Mechanism

The collimator mirror assembly is the most mechanically complex one after that of the xy stage. This mechanism is responsible for focusing the spectrograph (by moving the collimator mirror) and for dithering the fiber image (described below) in order to achieve precision flat-fielding calibrations. In addition, this assembly is able to align the collimator mirror precisely.

One of the major problems with existing fiber spectrographs is the inability to properly flat field an object. The reason for this is that the fiber image is round and, therefore, does not illuminate pixels perpendicular to the dispersion uniformly. Even a tiny amount of flexure which shifts the image on the CCD pixels creates a problem since there is no proper flat fielding on the CCD. In other words, calibration lamp exposures not taken at the same place and time as the object exposures might be imaged at a slightly different noncalibrated place on the detector.

In order to facilitate precision flat fielding, a mechanism has been devised which allows the profile of a fiber to be swept out over about a 10 pixel width (versus the normal 3.5 pixel FWHM). This mechanism oscillates the collimator mirror about an axis parallel to the spectral direction and generates a flat profile on the detector. The measured maximum flexure of the instrument is about one pixel, so any flexure that might occur between flat field and object exposure in the spatial dimension is overcome by this dithering process.

The dithering is accomplished by driving an eccentric via a Compumotor stepping motor but through a ten-to-one reduction bar. However, the mechanism as it stands is inadequate to produce a uniformly illuminated flat field over ten pixels. A cam of the appropriate shape was an option, although expensive and inflexible. A feature of the Compumotor system is that an entire sequence of move commands can be executed repetitively. This means that the rotation speed can be varied throughout a cycle to flatten out the projected epicyclic motion of the eccentric.

The collimator mirrors rest upon a set of plates each of which have a specific function: focus, dither, and alignment. The focus mechanism consists of two high-precision guide rails manufactured by New England Affiliates. These rails have approximately a 1 μm accuracy and were used because of their low profile which was needed to maintain compactness of the entire collimator mirror assembly. The focus plate is driven on roller screws (by NuTec) that have a 1 mm pitch and is driven by a Compumotor AX 57-102 microstepping motor with an Empire Magnetics brake. At the other end of the screw is an absolute rotary encoder manufactured by Parker (AR-23 with RS-422 interface). This encoder outputs 14 bits for every revolution. This translates into better than 1 μm accuracy for the entire focus system. The current configuration is such that one focus step is 12 μm.

Alignment of the entire collimator mirror assembly is possible through the use of push-pull screw sets at several locations. There are two plates one for fore-aft adjustment, another for side-to-side tilt adjustment, and lastly the entire assembly may be raised or lowered for proper centering.

3.4 Grating Rotator

The cell mounted gratings can easily be installed onto the grating rotator mechanism. On each grating there are four pins that define a four bit binary code system so that each and every grating used is uniquely identifiable by the instrument computer. The computer has a list of the available gratings and their characteristics. The only parameters that need to be set are the central wavelength and the order.

The grating angle is encoded by a single turn laser rotary encoder (Canon R1L) which yields adequate placment accuracy with the given gear train. The encoder has 81,000 steps per revolution and is electrically divided by a factor of 4 which yields 4 arcsec resolution. A Compumotor AX 57-51 microstepping motor was used for the rotation. A similar motor was used to actuate a cam that engages a brake to prevent unwanted grating rotation.

3.5 Shutter

Given the collimated beam size of about 150 mm, a commercially available high-quality shutter is just not available. The options for a shutter were rather limited. A curtain shutter located near the intermediate pupil (here the position of the grating) would have been ideal for uniform obstruction of the illumination at the detector. However, the size of the curtain would have been large and the mechanical logistics cumbersome.

The shutter design that we finally settled upon was one based upon a leaf diaphragm found in the large Kodak Aero-Ektar aerial camera. (Subsequently we found a supplier for these high-quality iris diaphragms, enough to keep Palomar well stocked for years to come.) These leaf diaphragms consist of 20 stainless-steel blades that open to a maximum of 88 mm. These leaves are mounted in a well designed brass housing. The leaves are interconnected near their pivot points through mechanical linkages. Onto one

of these leaves is attached an arm that is used to actuate the mechanism. We have attached to this arm a pull-pull double magnetic solenoid system. These solenoids take about 30 Volts dc for proper positive action. Shutter drive electronics are designed such that current is removed from the appropriate solenoid a few milliseconds after being pulsed. At each end of the travel of this linkage is a samarium-cobalt magnet that holds the steel linkage arm in place until the reverse operation occurs. Repeatability tests indicate that the shutter is reliable to 0.2 s, which is more than adequate for the observations with the Norris Spectrograph. The shutter assembly is located just before the field flattener of the Epps lens.

4. GUIDER CAMERAS

The Norris Spectrograph has two internal TV cameras that are used for observing. One of the TV cameras resides on the *xy* stage adjacent to the *z* head and is used for mapping the scale of the telescope focus as well as basic bright star acquisition. The other TV system is used primarily for guiding and, on occasion, field acquisition if this should become necessary.

The movable TV camera (or upper TV) is a commercially available frame transfer CCD camera system from Pulnix (TM-840N). This is a high-resolution CCD (800H $\times$490V) with 11.5$\times$13.5 μm pixels. There are electronics that allow integration on the chip up to 3 s and also serves as a scan converter with RS 170 video output. In practice, the camera is operated with about a 1-s integration. Before the detector there are focal reduction optics with a demagnification of about a factor of 3. This yields about 0.1 arcsec per pixel. With 1-s integrations and typical seeing a star of $V=18$ can easily be seen.

A fiducial has been established by the use of an electronic *xy* cursor inserted into the video by additional electronics manufactured by Colorado Video. In order to ensure the integrity of the position of this *xy* cursor, a reference cross hair is optically imaged onto the CCD by a small projection system that uses a beam splitter.

Guiding is accomplished by the use of a slow-scan Peltier cooled CCD camera system designed and was built in-house. This guide system consists not only of the CCD camera, but a focal plane reticle system, transfer optics, and a control computer which generates the error signals for the telescope. The 55 mm aperture for this system is located at a fixed position at one end of the *xy* stage and its entrance aperture on the *xy* stage can be seen in the photograph of Fig. 13. The focal reduction optics consist of a Zeiss *f*/2.8 150 mm lens that acts as a collimator and a 28 mm focal length Nikon camera lens. The resultant plate scale is about 73 μm per arcsec.

The CCD currently used is a TI virtual phase CCD (TI 4849) that has 590$\times$384 pixels, which are 22 μm in size. This yields 0.30 arcsec per pixel spatial sampling—more than adequate for guiding purposes. A slot for a 50$\times$50 mm^2 filter is available so that differential refraction between the guider and the fiber system can be partially compensated. The CCD is in an evacuated chamber and is cooled to a temperature between -85 and -65 °C (depending upon the ambient temperature) using a three-stage Marlow Peltier cooler. The hot plate of the largest cooler is soldered to a surface that is kept cool by the circulation of an ethylene glycol/water mixture through a heat exchanger located in the Cass cage.

The CCD is controlled using standard Palomar CCD electronics (see Gunn et al. 1987), which are, in turn, controlled by an Amiga 1000 computer. Menu driven software for controlling the CCD camera, displaying the images, and generating guiding errors, was written by Oke. The CCD can be operated in either full frame or frame transfer modes, and pixel binning is also available. It is anticipated that this system will be replaced by the new TV acquisition systems currently being developed for general Palomar use.

5. INSTRUMENT CONTROL COMPUTER

All of the functions of the Norris Spectrograph are controlled by a single computer. This is a VME-based 68020 system with a FORCE CPU 29X. The motor control software is written in C and operates under the PDOS operating system (Eyring Institute). A command executive similar to FORTH provides all the functions necessary to control the instrument. There are two modes for instrument control: *observing* and *engineering*; the latter command set is not normally available to observers. Commands are issued upon the FORCE console located in the data room of the 200-in. telescope. Files that contain the fiber setup information are generated on another computer and are transferred to the FORCE either by a dedicated serial link or by the use of Ethernet.

Information about the status of each fiber is kept on the hard disk of the FORCE and is updated if any changes occur. Fibers are lost only if an external force is applied to displace them from their known location, otherwise the computer controlled system can easily retrieve and move a fiber.

Additional boards on the VME bus are Ethernet, disk controllers (for floppy and Winchester disks), and a serial IO board (with six RS 232 ports). All communication to and from the spectrograph is converted to RS 422, encoded and multiplexed, and, via two coax lines, transferred to the other end.

6. SETUP SOFTWARE

Unlike a normal ground-based telescope and instrument, the Norris Spectrograph is not designed for extemporaneous observing. This was a conscious design criterion, to ensure that all preparations for observing were done prior to the observing session. A first step in preparing for an observing run is clearly to have an object list with accurate astronomical coordinates. This list is input to an interactive program that corrects for proper motion and precession, corrects for differential refraction over the 20 arcmin field of view of the *xy* stage, selects objects ac-

cording to priority (assigned by the astronomer), and attempts to assign fibers to objects based upon the specification of an appropriate guide star.

Applying an average precession value for all the object coordinates within the FOV of the Norris Spectrograph is insufficient. For example, over a 50-yr period differential precession can range from 1 to 2 arcsec at zero deg declination to over 10 arcsec at 60 deg declination. The transformation procedure used to convert coordinates from one equinox to another is accurate to about 1 arcsec per century.

A model for the atmosphere above Palomar is based upon the semiempirical formulation of Owens (1967) and is incorporated into the transformation pipeline. Differential refraction can be significant not only between the guider and the fiber system, but also between fibers. During extensive observations of the same field, an option exists to update each of the fiber positions at different zenith distances which helps correct for the effects of differential refraction.

Fiber setup software options include whether (a) to pair adjacent fibers at a specified position angle and distance for beam switched observations; (b) to automatically or manually select a guide star within specified ranges of variables; (c) to create a sequence of fiber setup files, one for each of the specified hour angles; (d) to assign fibers automatically or interactively; and to change parameters for the refraction corrections (atmospheric model). Another option is the ability to assign fibers to objects by dividing the stage into quadrants. This permits the *xy* stage to be arranged for up to four different setup files in the case where this type of assignment might be useful for fields with small numbers of objects to be observed such as might be found in distant clusters of galaxies.

A visualization of the *xy* stage arranged for an actual field is given in Fig. 14. The two banks of fibers are on the left and right and the fixed guider hole is indicated at the top. The abscissa is the *x* axis of the stage and the ordinate of this plot is the stage *y* axis. Units are in millimeters. High-priority objects are represented by black circles and low-priority objects by the open circles. Objects that have been assigned to a fiber are outlined by an open square. These types of plots are used in an interactive fashion on a computer workstation to view the object-to-fiber assignments prior to assembling the stage in this manner.

The ability to place fibers onto objects correctly depends not only upon the accuracy of the coordinates (α,δ) but also on the accuracy of the model of the focal plane. For approximately 30 min during twilight of the first night of an observing run, the plate scale[9] and rotation angle of the instrument must be determined for accurate stage astrometry. A linear model is assumed (rotation and translation) as the distortion that has been calculated to be negligible at the largest observable field angle. The process to determine the coefficients consists of obtaining the actual *xy* coordinates of bright stars found in galactic star clusters based upon the last best transformation coefficients. Once this process is complete the new transformation coefficients are determined by a linear least squares regression. Fitting residuals are approximately 0.2 arcsec. These new coefficients are then input into the aforementioned setup program which determines the correct values of the positions of the objects on the stage, assuming a specified guide star. Astronomical coordinates for the stars of the open clusters are taken from the *HST* Guide Star Catalog. Although these coordinates are only good to $\pm\sim 1$ arcsec for any individual star, the observation of ~ 20 stars averages out the supposedly random errors to an acceptable level.

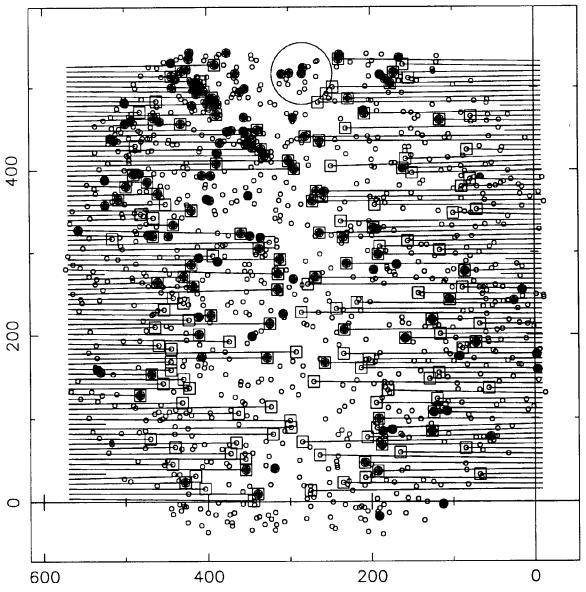

FIG. 14—A visualization of an actual field of faint galaxies with fiber assignments. The high-priority objects are the filled circles, and the lower-priority ones are the open circles. The objects that have been assigned fibers are outlined by a square and are connected by a line to the home (stowed) position of the fiber.

7. RESULTS

The instrument is being used for several distinctly different scientific programs. These include a redshift survey of faint galaxies, a radial velocity and metallicity survey of the stars in Galactic globular clusters, and also a radial velocity and metallicity study of globular clusters in external galaxies. Other programs are also in progress.

Sample spectra obtained with the Norris Spectrograph are presented in Fig. 15. The top panel shows a low-resolution spectrum of a high-redshift quasar found serendipitously during observations of faint galaxies. The exposure time was 7200 s. The lower spectrum of 3000 s is that of a globular cluster of the Andromeda Galaxy, M31. The noise of this latter spectrum is only a few percent, and some of the low contrast features such as the absorption features of the iron-peak elements are noted. The radial velocity of this cluster was measured to be -270 ± 8 km s^{-1}.

[9]The telescope focal length is temperature sensitive as expected given that the Serrurier truss is steel and the mirror is made out of Pyrex.

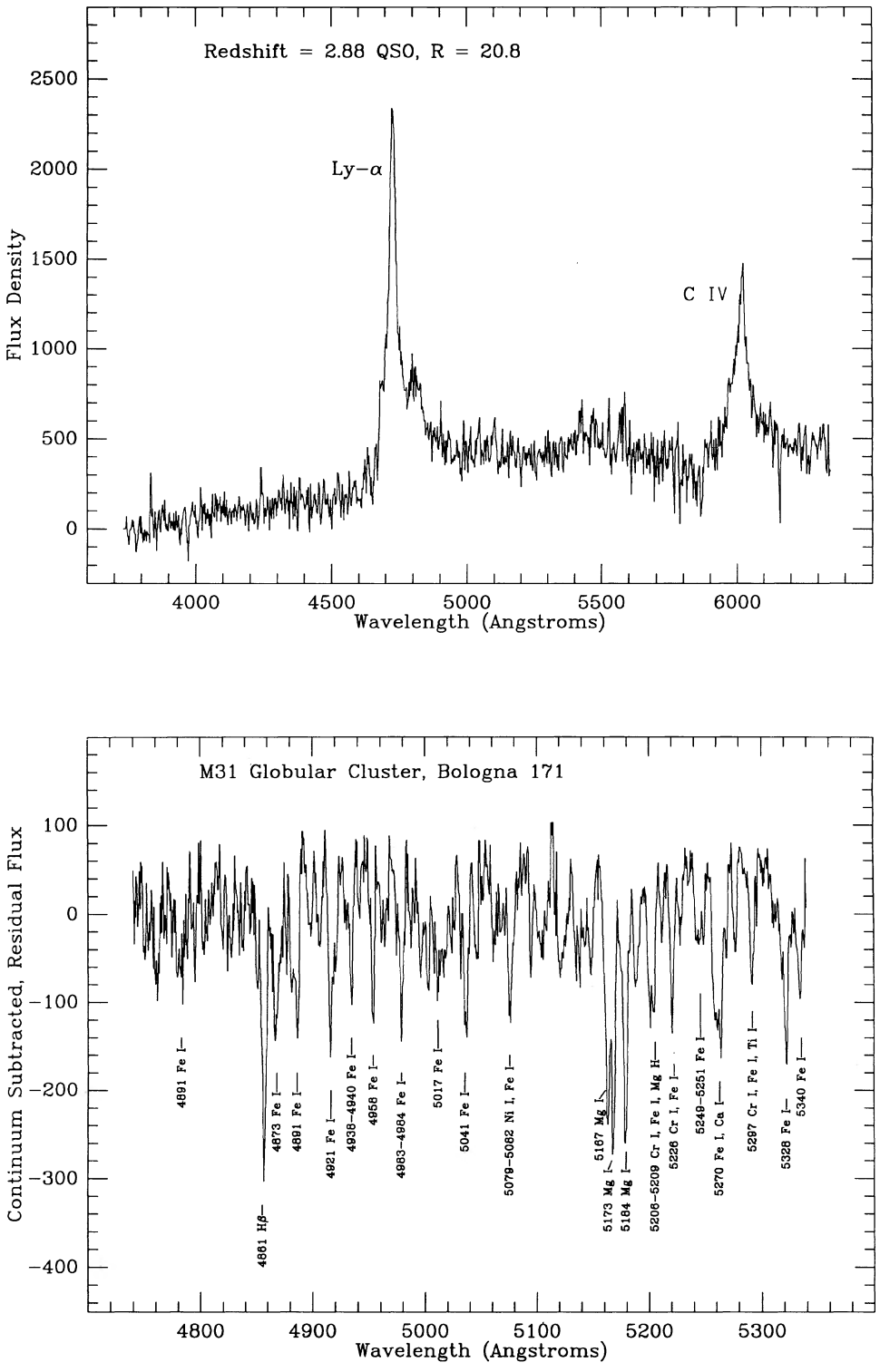

FIG. 15—Two spectra obtained with the Norris Spectrograph. The upper one is of a $z=2.88$ quasar found serendipitiously in a survey of faint galaxies. The other is a high-resolution spectrum of the M31 globular cluster Bo 171 and has a heliocentric radial velocity of -270 ± 8 km s^{-1}. The exposure times for these spectra were 7200 and 3000 s, respectively.

We would like to thank The Kenneth T. and Eileen L. Norris Foundation and especially Kenneth Norris for their kind support in the creation and use of this instrument. Not only did they make this instrument possible, but their interest in the science derived with it is much appreciated. The success of this project was due to the many people who made important contributions to the instrument's completion. In the area of software, D. C. Oke wrote the CCD control software for the Amiga; M. Strauss, A. Picard, T. Small, and Professor P. Seitzer all contributed to the off-line software. V. Nenow and G. van Idsinga both made valuable contributions to the electronics of the instrument. We would like to thank Professor Harland Epps and Gerard Pardahlan for their work with the camera lens of the Norris and Professor James Westphal for the use of his laboratory during the assembly and early testing of the instrument. Donald Loomis of Custom Optics did the optical work on the spherical collimator and the entrance window. Gaston Araya helped out in countless ways. We thank Professor James Gunn for illuminating discussions regarding flat-fielding techniques. Michael Doyle and John Henning of the Palomar Observatory staff provided uniquely invaluable service during the commissioning of the instrument. Finally, no Palomar paper would be complete without acknowledging the excellent assistance that Juan Carrasco has provided at The Hale Telescope over the decades.

REFERENCES

Barden, S. C. 1988, Fiber Optics in Astronomy (San Francisco, ASP)

Epps, H. 1989, Carnegie Observatories Preprint, unpublished

Epps, H. 1990, Proc. SPIE, Instrumentation in Astronomy VII, ed. D. L. Crawford (Bellingham, WA, SPIE), Vol. 1235, p. 550

Gunn, J. E., Emory, E., Harris, F. H., and Oke, J. B. 1987, PASP, 99, 518

Hamilton, D. 1990, Proc. SPIE, Instrumentation in Astronomy VII, ed. D. L. Crawford (Bellingham, WA, SPIE), Vol. 1235, p. 673

Oke, J. B., and Gunn, J. E. 1982, PASP, 94, 586

Owens, J. C. 1967, Appl. Opt., 6, 51

Ramsey, L. M. 1988, in Fiber Optics in Astronomy, ed. S. C. Barden (San Francisco, ASP), p. 26

von Rohr, M. 1899, Theorie und Geschichte des photographischen Objectivs (Berlin, Springer), p. 250